https://doi.org/10.5194/egusphere-2026-3720
Preprint. Discussion started: 7 July 2026

Assessing alignment-based chronology tuning for a 2000-year record of warm-water variability in Qeqertarsuup Tunua (Disko Bugt), West Greenland

Larissa Nora van der Laan[1], Ask Palnum Knudsen[1], Camilla Snowman Andresen[2], and Jens Hesselbjerg Christensen[1]

[1]Niels Bohr Institute, University of Copenhagen, Jagtvej 132, 2200 Copenhagen, Denmark
[2]Geological Survey of Greenland and Denmark, Øster Voldgade 10, 1350 Copenhagen, Denmark

Correspondence: Larissa Nora van der Laan (larissa.vdlaan@nbi.ku.dk)

Abstract. Chronological uncertainty limits the use of marine sediment cores for resolving the timing and coherence of late-Holocene ocean variability around Greenland. In this study, we apply two optimization methods to improve the chronological uncertainty of four sediment cores from Qeqertarsuup Tunua (Disko Bugt), West Greenland. Using the GISP2 temperature reconstruction as a reference series, we generate alignment-consistent age-model realizations with (i) Nelder-Mead optimization (NMO), which maximizes a resampled Pearson correlation coefficient (RPCC) and (ii) Dynamic Time Warping (DTW), which aligns sequential structure through non-linear time-axis adjustment. For individual cores, NMO generally yields higher RPCC values than DTW. However, when the adjusted records are merged into a Qeqertarsuup Tunua composite, DTW produces a substantially more coherent regional signal and a higher RPCC with GISP2 (0.77) than the NMO-based composite (0.36). To assess whether these improvements reflect genuine climate co-variability, we apply a phase-randomisation permutation test using 500 spectrally matched surrogate GISP2 series. Results are heterogeneous: DTW alignment is statistically significant for one core (Sullorsuaq, p=0.006), and NMO alignment is significant for another (Aasiaat 1, p=0.034), while neither method reaches significance for the other two cores. Restricting the composite to these two significant core and method combinations yields an RPCC of 0.83 with GISP2, outperforming both other composites. Applying both methods to a synthetic reference series also increases RPCC values, demonstrating that correlation gains can arise from alignment flexibility alone and underscoring the need for independent chronological constraints when interpreting tuned chronologies. Mean age offsets relative to the original models range from -99 to 41 yr for NMO and from -346 to $+190$ yr for DTW. We conclude that NMO can be useful for site-specific alignment and that the significance-filtered composite provides the most defensible regional reconstruction of Atlantic Water variability over the past 2000 years.

https://doi.org/10.5194/egusphere-2026-3720
Preprint. Discussion started: 7 July 2026

1 Introduction

The North Atlantic Oscillation (NAO) and Atlantic Multi-decadal Variability (AMV) are two dominant modes of climate variability that exert significant influence on the ocean-atmosphere system of the North Atlantic region. The NAO operates primarily on interannual to decadal time scales and affects weather patterns, temperature and precipitation, particularly in Europe and over Greenland (Hurrell, 1995; Hanna et al., 2013). The AMV, in contrast, is a coherent pattern of multi-decadal sea surface temperature (SST) variability in the North Atlantic, likely resulting from a combination of internal ocean dynamics and external forcings (Delworth and Mann, 2000; Schlesinger and Ramankutty, 1994). Together, these climate modes modulate the temperature and distribution of Atlantic-sourced waters along the West Greenland margin, particularly through their impact on the strength and positioning of the Irminger Current and the subpolar gyre system. Understanding the relative roles and interactions of the NAO and AMV is critical for assessing the oceanic heat transport to Greenland's marine-terminating glaciers, with implications for ice sheet stability, freshwater export, and broader climate feedbacks. However, the instrumental record is limited to the past 150 years and lacks the temporal length needed to resolve longer-term variability and to evaluate whether recent trends lie outside the range of natural variability. Marine sediment cores collected from the continental shelf and fjord systems near Greenland provide valuable archives for reconstructing past ocean conditions beyond the instrumental era. These paleoceanographic records can reveal important information about the long-term behavior of the combined NAO- and AMV-related ocean variability. However, their use is often constrained by chronological (age model) uncertainties, particularly in high-latitude settings where bioturbation, low sedimentation rates, and the scarcity of datable material challenge the construction of precise age models. As a result, reconstructions have faced challenges due to their lack of precise temporal alignment with climatic events.

In this study, we address chronological uncertainty in a set of four marine sediment cores, collected from Qeqertarsuup Tunua by Sermeq Kujalleq in West Greenland (see Fig. 1), a key meltwater-influenced region adjacent to the Greenland Ice Sheet. The cores contain information on Atlantic Water (AW) variability over the past 2000 years (the Common Era), as recorded in foraminiferal assemblages. The cores' age models are limited by low temporal resolution and large gaps between dating points, providing only coarse approximations of the true chronological frameworks. We present two methods for improving the age models, exploiting the well-established co-variability between oceanic and atmospheric systems on decadal timescales in the North Atlantic region (e.g. Yeager and Robson, 2017). The main idea behind our method is to use a well-dated independent record, in our case the Greenland Ice Sheet Project 2 (GISP2) record (Kobashi et al., 2011), as a temporal reference to align and optimize the age models of the marine sediment cores. These four proxy time series of AW variability all display similar multi-decadal to centennial trends, which are also evident in the temperature variability reconstructed from the ice core record. Because the ice core chronology is well constrained through annual layer counting, volcanic horizons and tephra layers (Meese et al., 1997; Vinther et al., 2006), we treat the ice core as a master timescale.

Using two distinct algorithms: (1) Nelder-Mead Optimization (NMO) based on the Resampled Pearson Correlation Coefficient (RPCC) and (2) Dynamic Time Warping (DTW), we match the marine proxy records to the ice core record. We identify shared features such as warming or cooling transitions and use these points of co-variability to tune the marine age mod-

https://doi.org/10.5194/egusphere-2026-3720
Preprint. Discussion started: 7 July 2026

els. This alignment explores age-model adjustments that reduce apparent chronological offsets among cores, which may arise from differences in sedimentation rates, depositional environments, or age-model uncertainty. The adjusted age models are treated as alignment-consistent realizations that facilitate regional synthesis under the assumption of a shared multi-decadal to centennial signal. The objective of this study is not to establish an absolute chronology for individual sediment cores, but to assess whether alignment-based age model adjustments can reduce apparent chronological offsets among multiple Qeqertarsuup Tunua records. Because the sediment records are of low to moderate resolution, we interpret alignment results primarily at multi-decadal to centennial timescales and do not use the tuned chronologies for event-scale synchronization. Beyond our specific region, these methods can be valuable in other regions where direct dating of proxy records is limited or ambiguous and where ocean-atmosphere or other coupling allows for meaningful synchronization of climate signals across different archives.

2 Data and Methods

This study modifies the age models of four sediment cores from locations in Qeqertarsuup Tunua (Disko Bugt): DA06-139G from Vaigat (Sullorsuaq) (Andresen et al., 2011), ACDC2014-001 from Isfjeldsbanken (offshore Ilulissat) (Wangner et al., 2018) and cores MSM343-300 (Perner et al., 2013; Ouellet-Bernier et al., 2014) and MSM343-310 (Perner et al., 2011; Lloyd et al., 2011) from Egedsminde Dyb (Aasiaat), see Fig. 1. From all these cores, we focus on the foraminiferal assemblages found in the sediment as a proxy for subsurface temperature. For the age model modification methods, we rely on the Greenland temperature reconstruction at the GISP2 site (Fig. 1; Kobashi et al., 2011). The time period chosen is where all cores overlap: 2000 BP to 1993 (where the present is defined as 1950).

2.1 Qeqertarsuup Tunua

Qeqertarsuup Tunua is a large (∼40,000 km^2) embayment in central West Greenland. It is characterized by a relatively shallow seabed, with depths ranging from 200–400 m (Jakobsson et al., 2020), reaching up to ∼1100 m in the glacially-formed Egedesminde Dyb trough (Andresen et al., 2011). Its oceanography is dominated by the West Greenland Current (WGC), a mix of the warm, saline Atlantic-sourced Irminger Current and the cold, low-salinity Arctic-sourced East Greenland Current (Andersen, 1981; Harff et al., 2007). The WGC enters the bay from the southwest and exits primarily through the Vaigat Strait in the north (Sha et al., 2014). The bay's surface waters are influenced by meltwater, icebergs, seasonal sea ice and low-salinity polar water from Baffin Bay, creating a dynamic environment with significant interannual variability in temperature, salinity and sea ice cover (Andersen, 1981).

2.2 Sediment Cores

The four sediment cores used in this study were recovered from different locations within Qeqertarsuup Tunua and each extends variably back into the Holocene. All cores were previously analyzed for lithology to assess depositional regimes and glacial inputs, including iceberg-rafted debris and plume sediments, along with a range of proxies to reconstruct water mass characteristics such as sea surface temperature and sea ice conditions (Andresen et al., 2011; Wangner et al., 2018; Perner

https://doi.org/10.5194/egusphere-2026-3720
Preprint. Discussion started: 7 July 2026

Table 1. Metadata for the sediment cores from Qeqertarsuup Tunua and the GISP2 ice core. N is the number of data points retained after filtering to the study period and, for the Aasiaat cores, after removing the no-foraminifera interval.

Core ID	Latitude	Longitude	Water depth (m)	N
DA06-139G (Sullorsuaq)	70°05.486′ N	50°53.585′ W	384	28
ACDC2014-001 (Isfjeldsbanken)	69°17.20′ N	51°16.20′ W	391	39
MSM343-300 (Aasiaat 1)	68°28.311′ N	54°00.119′ W	519	35
MSM343-310 (Aasiaat 2)	68°38.861′ N	53°49.493′ W	852	119
GISP2	72°36′ N	38°30′ W	–	1981

et al., 2011, 2013). To infer relative changes in subsurface West Greenland Current temperature, the cores were examined for variations in foraminiferal species assemblages. The temporal resolution of the temperature reconstructions varies among cores due to differing sedimentation rates and sampling resolution.

The DA06-139G core (Andresen et al., 2011), hereafter referred to as the Sullorsuaq core, was obtained at a depth of 384 m in the Vaigat Strait (Fig. 1). The temporal resolution from analyzing every 8th cm varies between 47 and 50 years (Andresen et al., 2011; Sha et al., 2014). Core ACDC2014-001, hereafter the Isfjeldsbanken core, was obtained approximately 15 km northwest from the mouth of the Ilulissat Isfjord at a water depth of 391 m (Wangner et al., 2018); it has a temporal resolution varying between 39 and 42 years, from samples taken every 5 cm. Core MSM343-300 (hereafter Aasiaat 1) and Core MSM343-310 (hereafter Aasiaat 2) were collected during a 2007 expedition by the Maria S. Merian (Harff et al., 2007). The Aasiaat 1 core has a temporal resolution varying between 4 and 9 years from samples taken every 4 cm (Perner et al., 2013). The Aasiaat 2 core has a temporal resolution varying between 12 and 15 years, also from samples taken every 4 cm (Perner et al., 2011).

The ages of the sediment cores were constrained with ^{210}Pb dating (approximately the last 150 years) and ^{14}C dating. This yields a number of date-depth combinations throughout the core: $N = 11$ over the 5500 years of the Sullorsuaq core, for example. An age model is then fitted to the calibrated element dates, usually assuming a linear relationship between core depth and age. This method contains inherent uncertainties due to the low number of dated levels per core. In this study we retain the original radiocarbon-based age models, calibrated with Marine13 (Reimer et al., 2013), to ensure comparability with existing Greenland marine records. Our focus is on relative refinement of age-depth models through stratigraphic alignment, not recalibration of absolute ages. The global marine reservoir age underlying the calibration curves changed from 405 ± 22 ^{14}C years in Marine13 (Reimer et al., 2013) to 550 ± 55 ^{14}C years in Marine20 (Heaton et al., 2020). Pearce et al. (2023) show that by recalibrating pre-bomb *Astarte* mollusks from Qeqertarsuup Tunua, the local correction (ΔR) shifts from $\Delta R \approx 140 \pm 35$ ^{14}C years (Marine13) to $\Delta R \approx 20 \pm 76$ ^{14}C years (Marine20). While this represents a large change in ΔR, the combined reservoir correction differs very little: ∼540 years in Marine13 versus ∼570 years in Marine20. This ∼30-year offset is far smaller than chronological uncertainties and the ±100–300 year adjustments from our optimization. This thus does not affect the stratigraphic structure or the conclusions of this study.

https://doi.org/10.5194/egusphere-2026-3720
Preprint. Discussion started: 7 July 2026

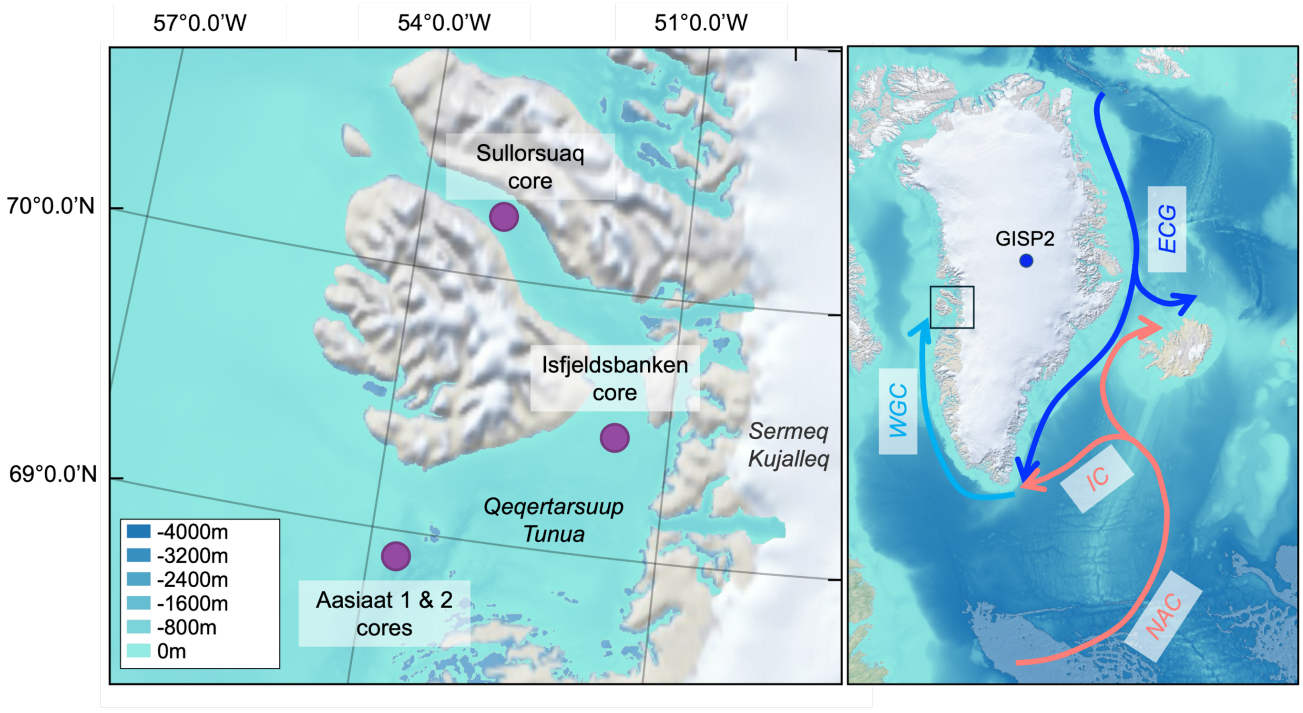

Figure 1. Visualization of Qeqertarsuup Tunua with dots indicating the location of the four sediment cores and the GISP2 ice core. Arrows indicate the currents around Greenland: WGC = West Greenland Current, EGC = East Greenland Current, IC = Irminger Current, NAC = North Atlantic Current. The bathymetry shown is relative to mean sea level. Spatial data provided by the QGreenland dataset (Moon et al., 2023).

2.3 GISP2

The GISP2 temperature reconstruction (Kobashi et al., 2011) was developed from an ice core from the Summit region of central Greenland (72°36′N, 38°30′W; 3200 m a.s.l.). The core spans the Holocene (ca. 11,600 years). This high-resolution reconstruction is based on the fractionation of argon and nitrogen isotopes in trapped air bubbles, linked to depth temperature gradients in firn layers (Kobashi et al., 2008). These measurements are combined with borehole temperature data to incorporate both decadal-to-centennial and low-frequency climate signals. Using a firn densification and heat diffusion model, the method provides a detailed surface temperature history spanning 11,580 BP to 1993. For the current study, we focus on the past 2000 years, comprising 1981 data points.

2.4 Data Selection

Benthic foraminifera are particularly sensitive to environmental changes and serve as a proxy for ocean current change (Murray, 1991; Perner et al., 2011). Especially in high northern latitudes, the distribution of some species is governed to a large extent

https://doi.org/10.5194/egusphere-2026-3720
Preprint. Discussion started: 7 July 2026

by water mass characteristics such as temperature and salinity (e.g. Rytter et al., 2002; Sejrup et al., 2004; Lloyd et al., 2011). As Wangner et al. (2018) note, there is a strong correlation between their proxy bottom water temperature records and the Kobashi et al. (2011) air temperature reconstruction. The current study bases its methodology on this relationship between the abundance of warm-water foraminiferal assemblages and air temperature. However, the two Perner cores from southern Qeqertarsuup Tunua show long intervals with no foraminifera presence in the sediment: the Aasiaat 1 core between approximately 2001–1350 CE (i.e., post-600 BP under the original age model), and the Aasiaat 2 core between approximately 2005–1350 CE (i.e., post-600 BP under the original age model). Because temperature continues to vary while no foraminifera are present, these intervals disrupt the trend-matching methods and they have therefore been excluded. The number of data points and time span retained per core are detailed in Table 1.

2.5 Resampled Pearson Correlation

The different resolutions of the datasets (see Table 1) necessitate resampling to calculate the degree of relationship between ice-core and sediment-core data. To calculate a Pearson correlation, the GISP2 time series is resampled at the corresponding integer timestamp of the sediment core data. A Pearson correlation is then calculated between these two same-length series A Pearson correlation is then calculated between these two same-length series. This value is not a true measure of the correlation between the sediment-core time series and the full GISP2 temperature record, but between the sediment-core time series and the resampled GISP2 series. It serves as an approximation of the degree of co-variability between the datasets and is used to gauge whether a shift in the sediment core age model is beneficial. We refer to this quantity as the Resampled Pearson Correlation Coefficient (RPCC):

$$\mathrm{RPCC} = \frac{\sum_{i=1}^{n}(X_i - \bar{X})(Y_{\mathrm{resampled},i} - \bar{Y}_{\mathrm{resampled}})}{\sqrt{\sum_{i=1}^{n}(X_i - \bar{X})^2 \sum_{i=1}^{n}(Y_{\mathrm{resampled},i} - \bar{Y}_{\mathrm{resampled}})^2}}.$$

Here, X_i represents the foraminiferal data at a given time point and $Y_{\mathrm{resampled},i}$ represents the GISP2 temperature data resampled to the same number of points as the foraminiferal data, at the corresponding integer timestamps.

2.6 Nelder-Mead Optimization Method

The first method to optimize the sediment core age models is the Nelder-Mead Optimization method (NMO) (Nelder and Mead, 1965), which attempts to find an adjusted set of sample ages that maximizes the RPCC between the foraminiferal concentration data and GISP2 temperature data. NMO is a non-gradient method of optimization, commonly used to detect extrema in a function of many variables (Chelouah and Siarry, 2003). Assuming a linear relationship, the age model at which the RPCC between the sediment core and GISP2 data is highest is considered the most reliable.

All data are first normalized via min-max scaling and only data before 1950 BP are retained. After calculating the RPCC between the resampled GISP2 data and the sediment core data using the original age model, the chronology is initially perturbed by multiplying it with scaling factors between 0.9 and 1.1. These scalings are used solely to provide different starting points

https://doi.org/10.5194/egusphere-2026-3720
Preprint. Discussion started: 7 July 2026

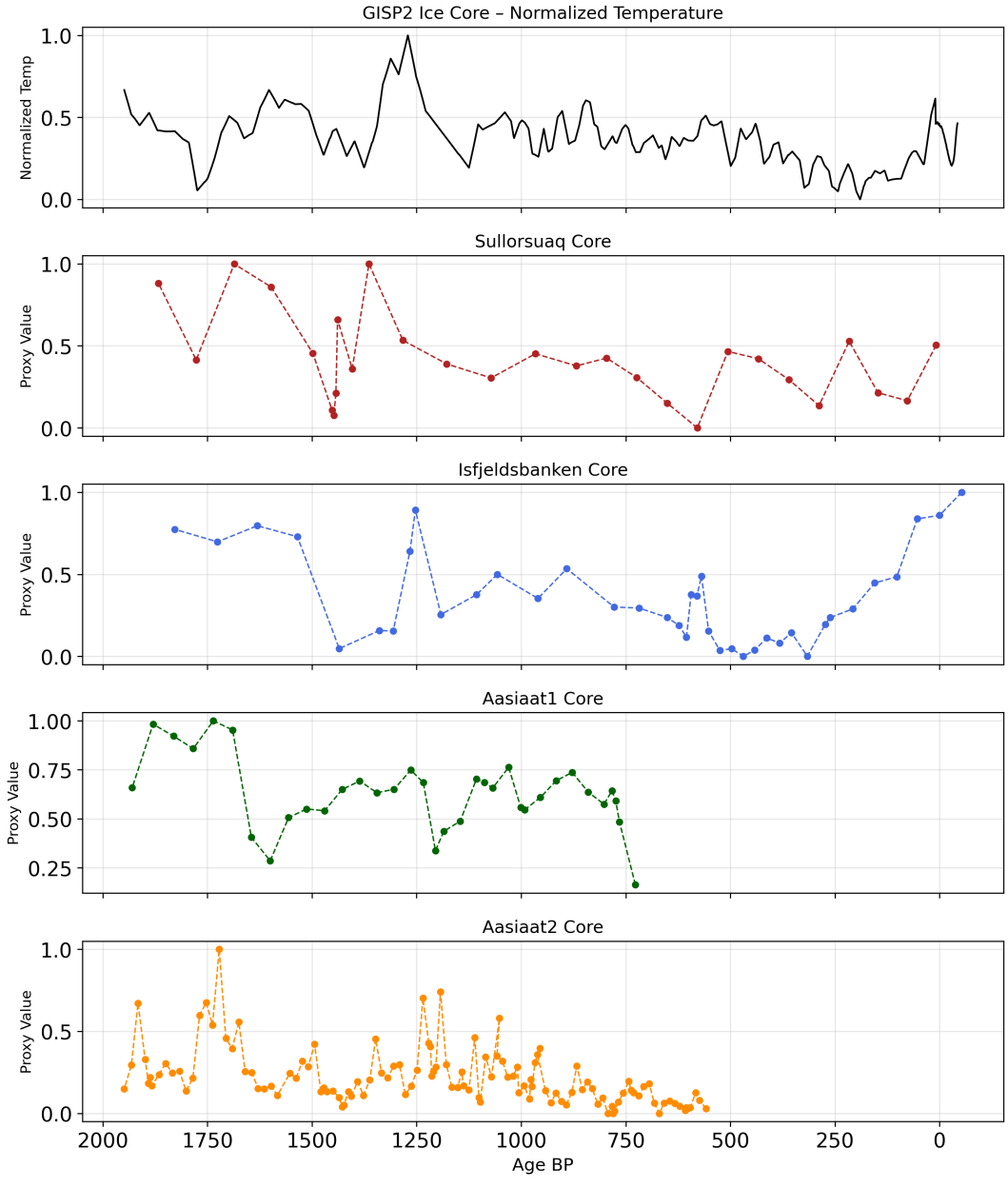

Figure 2. Qeqertarsuup Tunua sediment core foraminiferal concentrations with their initial age models and GISP2 reconstructed Greenland temperature. Year 0 corresponds to the Gregorian year 1950.

https://doi.org/10.5194/egusphere-2026-3720
Preprint. Discussion started: 7 July 2026

for the NMO and do not represent final age model solutions. From each of these initial conditions, the Nelder-Mead algorithm iteratively adjusts the ages of individual data points in order to maximize the RPCC, under the constraint that the chronological order of the sediment core is preserved. The optimization bounds allow each age point to shift by up to ± 1000 years relative to its original value, providing a wide exploration window while remaining physically plausible given the typical chronological uncertainties of these cores. As a result, the optimized age model is not a uniform scaling of the original chronology: individual sample ages may shift forward or backward in time relative to the original model, while the overall stratigraphic order remains intact.

This method of (1) shifting the chronology, (2) resampling the GISP2 temperature record and then (3) calculating the RPCC is repeated using a Nelder-Mead optimization routine (Nelder and Mead, 1965), with the aim of yielding the highest possible RPCC. As the four sediment cores have varying resolutions (28, 39, 35 and 119 points respectively; see Fig. 2), the degrees of freedom differ for each core and the computational demand varies correspondingly. The Aasiaat 2 core routine is run for 5250 iterations, while the other three cores are run for 21,000 iterations. Output from the optimization routine includes the RPCC per iteration, the adjustments of each datum from the initial age model and the mean adjustment in years. This mean adjustment is referred to as the age model skew, describing the average offset of the optimized ages relative to the original age model. Because individual data points may shift by different amounts, the skew reflects a general tendency toward older or younger ages rather than a uniform correction.

2.7 Dynamic Time Warping

The second age model optimization approach uses Dynamic Time Warping (DTW) (Salvador and Chan, 2007). DTW is capable of aligning two time series with substantially different temporal resolutions by allowing non-linear temporal shifts that best match their underlying trends. Here, we use DTW to detect the optimal correspondence between the low-resolution foraminiferal proxy records and the high-resolution GISP2 temperature record. As in the NMO approach, the data are normalized and only data points corresponding to the target period (years before 1950) are retained.

The DTW algorithm computes a warping path: a set of paired indices where each element of the foraminiferal proxy record is optimally aligned with one or more points in the GISP2 dataset. A mapping is constructed such that each sediment core index j is linked to the set of ice core indices i that the DTW deems to correspond to it. The optimized age of each sediment core sample is then calculated as the arithmetic mean of the corresponding ice core ages, rounded to the nearest integer year. The resulting age model adjustments (age model skew) are then quantified.

It is important to note that, unlike NMO, DTW has as many degrees of freedom as there are data points in the longer series (here, 1981 GISP2 points), meaning it can in principle achieve high alignment scores against any smooth series. This property is consistent with the high RPCC values obtained against the random time series (Section 2.8) and reinforces the need for the significance testing described in Section 2.9.

https://doi.org/10.5194/egusphere-2026-3720
Preprint. Discussion started: 7 July 2026

2.8 Random Time Series Application

To assess the specificity of both adjustment methods, they are also applied to a synthetic time series. A randomly generated time series at the GISP2 temporal resolution ($N = 1981$) is constructed using an online time series generator (Becker and Blascheck, 2024), producing a dataset with similar noise characteristics, amplitude and trends to a plausible ice core record. The Nelder-Mead and DTW routines are subsequently applied to the sediment core data and this random dataset, hereafter referred to as the RTS (random time series).

2.9 Phase-Randomisation Permutation Significance Test

To assess whether the observed RPCC improvements are statistically significant, rather than arising purely from the degrees of freedom available to the optimization, we apply a phase-randomisation permutation test (Räth and Monetti, 2009). For each core and each method, we generate 500 surrogate GISP2 series that preserve the amplitude spectrum of the real GISP2 record (and thus its autocorrelation structure) but have fully randomised Fourier phases. These surrogates are spectrally indistinguishable from GISP2 yet share no phase relationship with the sediment cores, providing a null distribution of optimised RPCC values achievable by alignment flexibility alone. Both NMO and DTW are then applied to each core against each surrogate and the resulting optimised RPCC values form the null distribution. The empirical p-value is defined as the fraction of surrogates whose optimised RPCC meets or exceeds the real optimised RPCC. This test is more rigorous than the single-RTS comparison in Section 2.8: it uses 500 spectrally matched surrogates and produces a full null distribution rather than a single reference value.

2.10 Merging into composite

To assess regional coherence and reduce site-specific noise, we combine the optimized age models from the four sediment cores into merged time series. For each optimization method, sediment core values are reassigned to their optimized ages and merged into a single composite dataset. This procedure retains the order of each core's observations but aligns them within a common chronological framework, enabling direct comparison across sites. The rationale for merging lies in the physical similarity of the sites: all four cores are located within Qeqertarsuup Tunua and record variability in the advection of Atlantic-derived waters into Baffin Bay. Although each core contains site-specific noise and chronological uncertainty, the underlying signal of bottom-water temperature variability is expected to be coherent at the regional scale. By merging optimized chronologies, we enhance the expression of this common signal and provide a stronger basis for comparison with the GISP2 ice-core record. We also create a composite restricted to the two core/method combinations that pass the permutation significance threshold ($p<0.05$): Sullorsuaq (from DTW) and Aasiaat 1 (from NMO) (Fig. 7).

2.11 Interpretation scope and assumptions

The alignment methods applied here assume that the Qeqertarsuup Tunua marine proxy records and the Greenland temperature reconstruction share a coherent expression of regional climate variability at multi-decadal to centennial timescales. The ad-

https://doi.org/10.5194/egusphere-2026-3720
Preprint. Discussion started: 7 July 2026

justed age models are therefore treated as alignment-consistent realizations that reduce apparent chronological offsets among records under this assumption. They are not used to infer event-scale synchronicity and they do not replace independent chronological constraints from radiocarbon and element dating.

3 Results

The NMO yields substantial improvements in the alignment between the sediment core data and the GISP2 temperature records. Table 2 shows the RPCC values for each core before and after adjustment against the GISP2 ice core data. The Sullorsuaq core shows the highest improvement, with an optimized RPCC of 0.900, up from an initial 0.293. The Aasiaat 1 core, despite its initial negative correlation, also sees a significant improvement. Of the four sediment cores, Aasiaat 2 is the only one for which the optimized NMO RPCC does not indicate a strong fit with GISP2. Using the Sullorsuaq core as an example, Fig. 3 shows the RPCC per optimization iteration and the age model yielding the maximum RPCC. The RPCC values vary widely due to the many degrees of freedom in the optimization. The local function optima, indicated in Fig. 3, vary in their RPCC, with some solutions yielding lower scores than the initial RPCC of 0.293. This is a consequence of the wide initial scaling range, which can suggest starting points that are not viable. The highest RPCC solution occurs with a scaling constant of 0.95, indicating that the optimized realization implies younger ages on average than the initial age model. Overall, a peak occurs around a skew of -44 years (Fig. 4), indicating that many high-RPCC solutions cluster around this value.

Optimizing the Sullorsuaq age model with DTW yields an optimized RPCC of 0.839, compared to the initial RPCC of 0.293 (Fig. 5). The mean skew for this solution is -47 years, consistent with the NMO result. However, in contrast to NMO, the warping path could only be established while allowing a skew magnitude of up to 600 years, meaning the per-point skew ranges from -502 to $+370$ years, neither imposing a systematic young or old bias.

Overall, for individual cores, NMO frequently achieves higher or comparable RPCC values compared to DTW, reflecting the local optimization of each core's chronology relative to GISP2. DTW generally results in slightly lower individual correlations (e.g. 0.66 vs. 0.739 for Isfjeldsbanken). Both NMO and DTW also improve RPCCs against a synthetic random time series, in some cases yielding values exceeding 0.7 (Table 3), underscoring the flexibility of both methods to force alignment even where no physical covariance exists.

3.1 Phase-Randomisation Permutation Significance Test

To assess whether the observed RPCC improvements could arise from alignment flexibility alone instead of a genuine shared climate signal, we apply a phase-randomisation permutation test (Section 2.9) to all four cores and both methods. Results are summarised in Table 4 and illustrated in Fig. 6.

The results are heterogeneous across cores and methods, which is in itself informative. For the Sullorsuaq core, the DTW improvement is statistically significant ($p = 0.006$), with the real RPCC of 0.839 exceeding the null 95th percentile of 0.729. The NMO improvement for Sullorsuaq approaches but does not reach significance ($p = 0.066$). For the Aasiaat 1 core, the pattern is reversed: the NMO improvement is significant ($p = 0.034$, real RPCC 0.878 versus null 95th percentile 0.871), while

https://doi.org/10.5194/egusphere-2026-3720
Preprint. Discussion started: 7 July 2026

the DTW result is not ($p = 0.616$). This reflects the low DTW RPCC for that core (0.396), which lies well within the null distribution. For Isfjeldsbanken and Aasiaat 2, neither method yields significant results. Notably, the Isfjeldsbanken DTW null 95th percentile (0.857) substantially exceeds the real DTW RPCC (0.656), indicating that surrogate GISP2 series routinely outperform the real record for this core under DTW alignment, consistent with the high DTW degrees of freedom discussed in Section 2.7.

The lack of significance for some core and method combinations reinforces that the permutation test captures method-specific alignment flexibility rather than the presence or absence of a regional climate signal. Cores and methods where significance is achieved provide stronger evidence that the aligned age model reflects a genuine common signal with GISP2.

3.2 Merging into Composite

When the optimized chronologies are merged into method-specific composite time series (Fig. 7), DTW outperforms NMO. The merged DTW chronology yields a markedly higher RPCC with GISP2 (0.77) than the merged NMO chronology (0.36). The merging approach also reveals that NMO produces strong individual correlations but limited cross-core coherence, whereas DTW explicitly aligns structural variability across records. DTW therefore yields a more temporally coherent composite under the alignment assumption. The third composite, composed of only the cores whose tuned results pass the permutation significance threshold (p<0.05), yields a composite RPCC with GISP2 of 0.83. The improvement over the all-core DTW composite reflects the removal of Isfjeldsbanken and Aasiaat 2, whose optimised age models are not distinguishable from surrogate-driven alignment. Using results from both methods in the filtered composite illustrates that neither method is universally superior. In practice, we recommend using the significance-filtered composite as the primary regional synthesis.

Core	Initial RPCC	Optimized RPCC (NMO)	Optimized RPCC (DTW)
DA06-139G (Sullorsuaq)	0.293	0.900	0.839
ACDC2014-001 (Isfjeldsbanken)	0.319	0.739	0.656
MSM343-300 (Aasiaat 1)	−0.021	0.927	0.681
MSM343-310 (Aasiaat 2)	0.032	0.375	0.610

Table 2. Initial and post-optimization RPCC values between the sediment-core and GISP2 time series.

Core	Initial RPCC	Optimized RPCC (NMO)	Optimized RPCC (DTW)
DA06-139G (Sullorsuaq core)	0.049	0.653	0.691
ACDC2014-001 (Isfjeldsbanken core)	0.036	0.410	0.504
MSM343-300 (Aasiaat 1 Core)	-0.104	0.778	0.859
MSM343-310 (Aasiaat 2 Core)	-0.0641	0.374	0.687

Table 3. Initial and post optimization RPCC values between the sediment core- and the random time series.

https://doi.org/10.5194/egusphere-2026-3720
Preprint. Discussion started: 7 July 2026

Core	Real RPCC (NMO)	p (NMO)	Real RPCC (DTW)	p (DTW)
DA06-139G (Sullorsuaq)	0.865	0.066	0.839	0.006^{**}
ACDC2014-001 (Isfjeldsbanken)	0.724	0.144	0.656	0.634
MSM343-300 (Aasiaat 1)	0.878	0.034^{*}	0.396	0.616
MSM343-310 (Aasiaat 2)	0.334	0.372	0.610	0.294

Table 4. Phase-randomisation permutation test results for all four cores and both methods ($N = 500$ surrogates). p-values are empirical (fraction of surrogate RPCC values $\geq$ the real optimised RPCC). $^{*}p < 0.05$, $^{**}p < 0.01$.

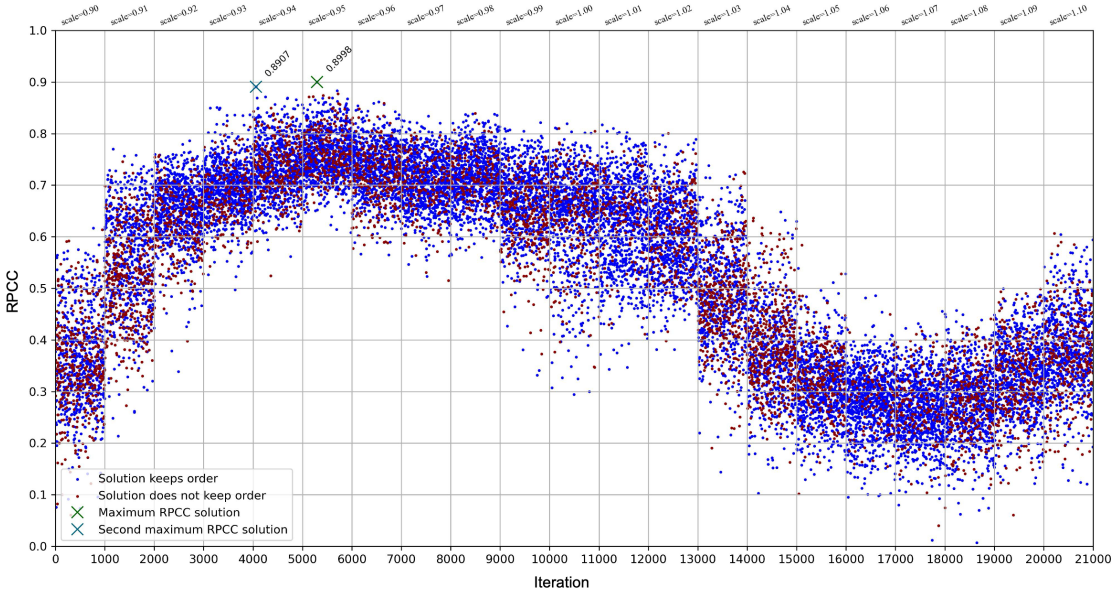

Figure 3. Scatter plot of the 21,000 optimized age models for the Sullorsuaq sediment core against the GISP2 time series. The iteration index is shown on the lower horizontal axis, with different age scalings indicated on the upper horizontal axis. The four local maximum RPCC scores are marked with an X.

4 Discussion

Both optimization methods substantially improve the apparent agreement between sediment core chronologies and the GISP2 ice core temperature record, but in different ways. NMO excels in maximizing the local fit for each individual record. This is advantageous for site-specific reconstructions, where aligning a single proxy record with an atmospheric reference series may provide the most accurate chronology. However, because the NMO operates independently on each record, the resulting chronologies can diverge between sites, producing poor alignment when merged into a regional composite (Fig. 7). DTW, in contrast, prioritizes alignment of shared structural variability, preserving chronological consistency across cores. While it is

https://doi.org/10.5194/egusphere-2026-3720
Preprint. Discussion started: 7 July 2026

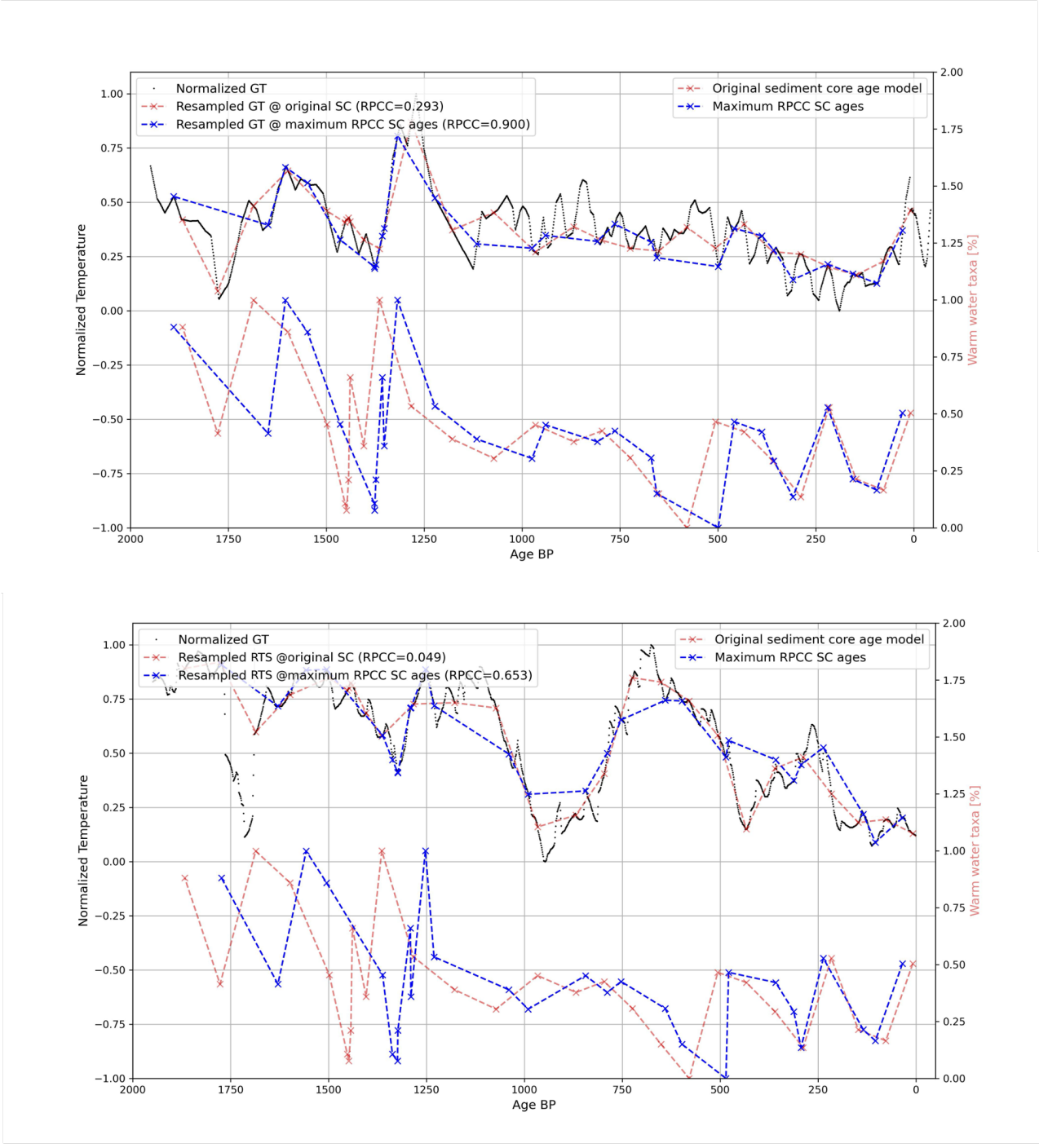

Figure 4. Nelder-Mead Optimization results for the Sullorsuaq core against the GISP2 time series (top panel) and a random time series (bottom panel).

https://doi.org/10.5194/egusphere-2026-3720
Preprint. Discussion started: 7 July 2026

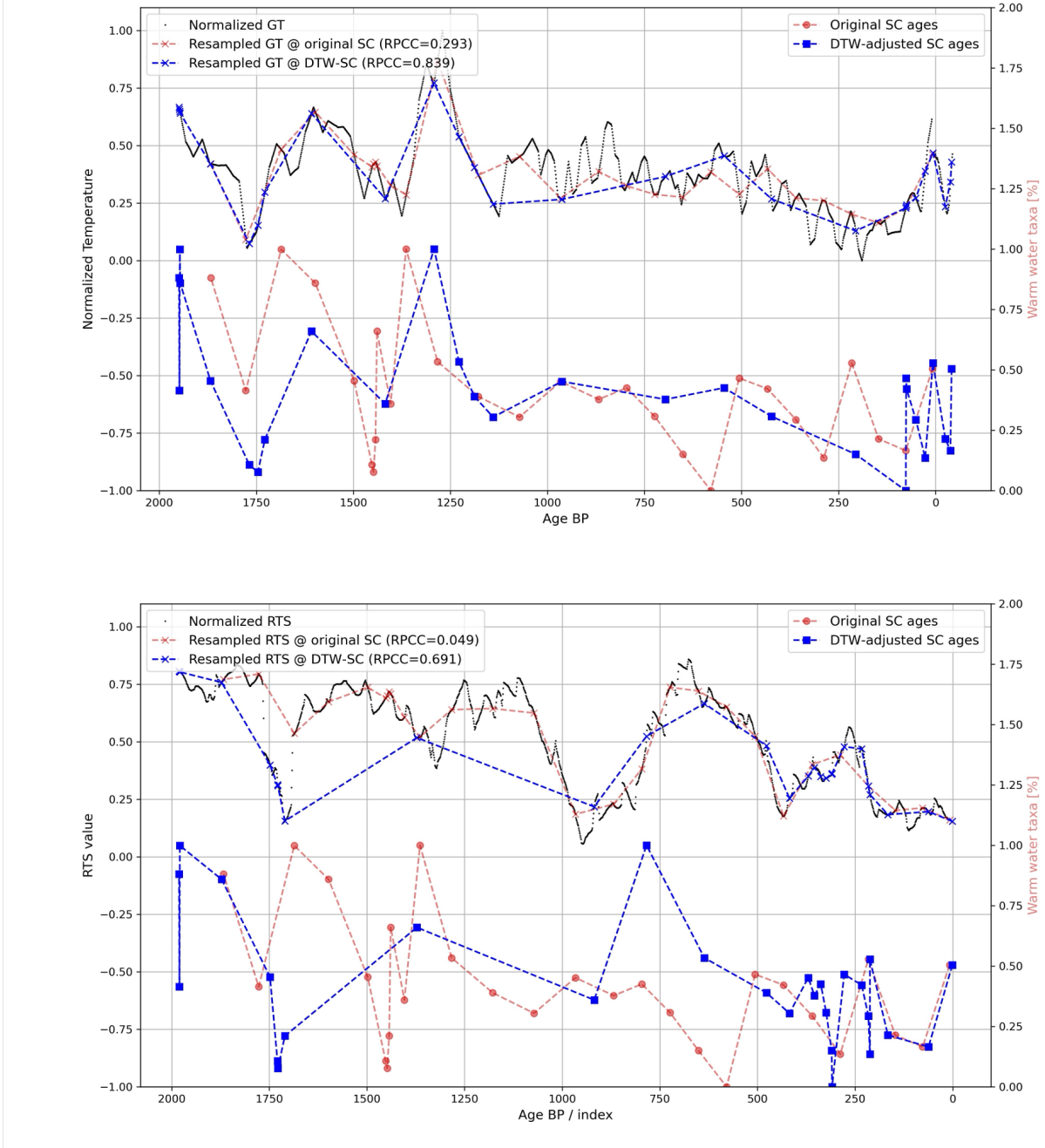

Figure 5. Dynamic Time Warping results for the Sullorsuaq core against the GISP2 time series (top panel) and a random time series (bottom panel).

https://doi.org/10.5194/egusphere-2026-3720
Preprint. Discussion started: 7 July 2026

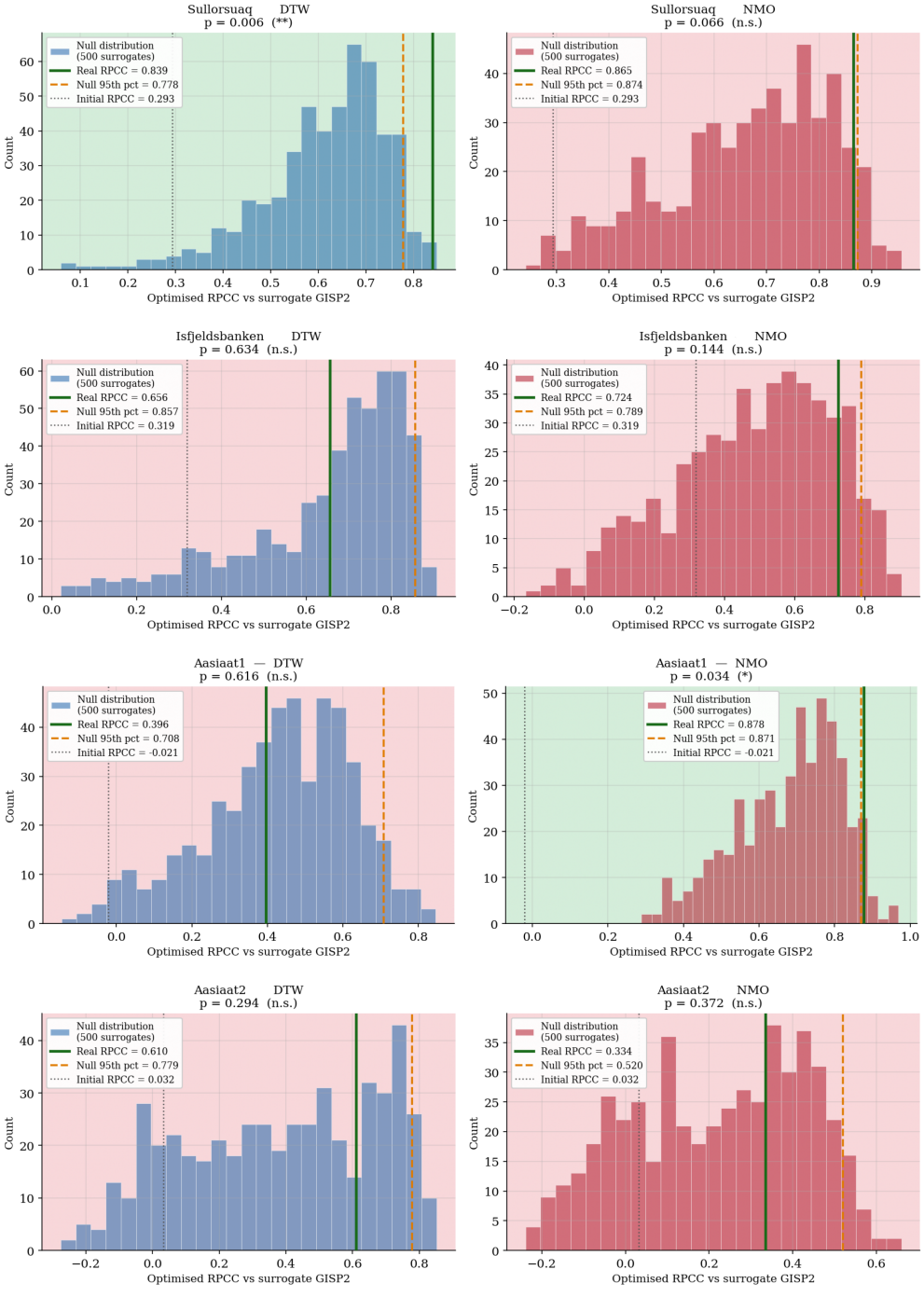

Figure 6. Phase-randomisation permutation test results for all four cores. Each panel shows the null distribution of optimised RPCC values obtained by applying DTW (blue) or NMO (red) to 500 phase-randomised surrogate GISP2 series. The green vertical line marks the real optimised RPCC. The orange dashed line marks the null 95th percentile. The green panel background indicates $p < 0.05$, the red indicates $p \geq 0.05$.

https://doi.org/10.5194/egusphere-2026-3720
Preprint. Discussion started: 7 July 2026

Figure 7. Merged composite optimized age models for all cores, using the Nelder Mead Optimization method (top panel) and dynamic time warping (middle) operating on GISP2 ice core data. The bottom panel shows a composite using both methods, restricted to results that pass the permutation significance threshold (p<0.05). The differently colored data points indicate from which core the value is initially.

https://doi.org/10.5194/egusphere-2026-3720
Preprint. Discussion started: 7 July 2026

applied to each core individually, its emphasis on aligning sequential structure produces age models that are more consistent across sites when merged. This property is reflected in the much stronger correlation of the DTW-merged series with GISP2 compared to the NMO-merged series and in the visual appearance of concentrated peaks and valleys in the composite record (Fig. 7). The added filter of the significant testing strengthens the case for the use of the multi-method composite record. Such a merged multi-core record is especially useful for regional climate teleconnection studies focusing on larger patterns rather than site-specific variability.

The fact that both optimization approaches also yield strong apparent correlations with a randomized time series emphasizes the importance of independent chronological constraints. Without tephrochronology, layer counting, or other absolute markers, optimization methods may exploit statistical flexibility to force alignments. Nevertheless, the fact that multiple Qeqertarsuup Tunua records respond similarly under alignment to the same reference series suggests that the adjustments are not purely idiosyncrasies of a single core. We therefore treat the tuned chronologies as alignment-consistent realizations that may reduce apparent chronological offsets under the assumption of shared regional variability, while emphasizing that correlation improvements alone do not constitute independent validation of coupling or synchronicity.

The phase-randomisation permutation test results illuminate the extent to which each core's RPCC improvement reflects a genuine signal rather than alignment flexibility. The heterogeneous outcomes across cores and methods are themselves informative. DTW is statistically significant only for Sullorsuaq, where the real RPCC (0.839) clearly exceeds what phase-matched surrogates can achieve. For Isfjeldsbanken, the DTW null distribution has a 95th percentile of 0.857, well above the real DTW RPCC of 0.656, confirming that DTW's improvement for that core is largely an artefact of its high degrees of freedom. The contrast between NMO and DTW in Aasiaat 1 is particularly instructive: NMO is marginally significant ($p = 0.034$) while DTW is not, consistent with DTW's tendency to spread adjustments across the entire record in a way that may not preferentially reflect a shared signal. For Aasiaat 2, neither method achieves significance, which is consistent with the low NMO RPCC (0.334) and the high DTW skew (-346 years) that together suggest chronological alignment is poorly constrained for this core. Taken together, the permutation results support a cautious interpretation: the methods can identify cores and configurations where alignment improvements are unlikely to be spurious, but they also reveal cases where the optimization flexibility dominates the result.

The contrasting skew values illustrate the methods' fundamental differences. NMO's focus on dominant features can cause relatively large negative shifts, as observed for Aasiaat 1 (-99 years), where the algorithm pulls the chronology earlier to optimize the fit to prominent peaks and valleys. DTW, applied separately to each core, aligns the entire sequence of variability while preserving the order of observations. Rather than shifting the record as a whole, DTW distributes adjustments across the series, progressively stretching or compressing time intervals to minimize local mismatches. This cumulative process can generate large positive average shifts, as seen for Aasiaat 1 ($+190$ years), when repeated small lags relative to the ice core reference build up across the record. These differences emphasize that skew magnitude and direction are method-dependent outcomes: NMO tends to overfit locally, while DTW enforces sequential consistency, leading to regionally more coherent but sometimes strongly shifted chronologies. Skew values should therefore be interpreted cautiously, not as absolute corrections but as reflections of the optimization strategy.

https://doi.org/10.5194/egusphere-2026-3720
Preprint. Discussion started: 7 July 2026

Finally, despite these improvements, some inherent data limitations remain. The low resolution of the original sediment core data limits the accuracy of the new age models. Additionally, the assumption of a linear relationship between bottom water temperatures in Qeqertarsuup Tunua and GISP2 inland temperatures may not fully capture the complexity of regional climate dynamics, missing non-linear feedbacks, lags and more complex interactions among the atmosphere, ocean and cryosphere. Optimized models should therefore be used as interpretive aids rather than as definitive chronologies. Nevertheless, the new composite record of warm-water conditions in Qeqertarsuup Tunua provides a more robust relative framework than the original weakly constrained models, making it valuable for identifying broad phases of oceanographic change and for comparison with independently dated climate archives.

5 Conclusions

Precise age models for reconstructions of the West Greenland Current are essential for global research initiatives aimed at reconstructing and understanding climate variability over the past 2000 years, such as the PAGES 2k Consortium. The WGC influences regional ocean circulation, sea ice extent and Greenland Ice Sheet dynamics, all components of past climate variability. High-resolution, well-dated records help identify the timing and mechanisms of climate events, improving our understanding of climate teleconnections and the sensitivity of the North Atlantic system to external forcings.

This study demonstrates the potential of optimization methods to refine the age models of sediment cores from Qeqertarsuup Tunua. By aligning these proxies with the well-dated GISP2 temperature reconstruction, significant improvements in the apparent agreement between sediment core proxies of bottom water conditions and the Greenland ice core temperature record can be achieved. NMO yields superior fits for individual cores, making it well suited for site-specific studies. DTW generates regionally coherent age models that maximize the combined signal of multiple records and is therefore preferable for regional syntheses. The strong performance of both methods against a random time series highlights the importance of retaining independent chronological constraints such as tephra layers, volcanic horizons or radiocarbon ages. The phase-randomisation permutation test provides a formal quantification of this risk. Optimized chronologies should therefore be viewed as refinements, not replacements, of existing age models.

For regional syntheses of Qeqertarsuup Tunua sediment cores and their integration with Greenland ice cores, we recommend the use of the significance-filtered merged composite. For single-core studies, NMO may remain a useful tool provided age shifts remain within stratigraphic uncertainty bounds. Looking ahead, the integration of independent tephrochronological markers would provide a powerful test of whether the alignment-inferred age shifts correspond to real depositional events and would further constrain the range of permissible age model realizations. The methods and open-source code presented here are directly transferable to other regions where proxy dating is limited and ocean-atmosphere coupling supports cross-archive alignment.

https://doi.org/10.5194/egusphere-2026-3720
Preprint. Discussion started: 7 July 2026

Code and data availability. The code used for the alignment experiments (NMO and DTW, including the phase-randomisation significance test) and the processed time series used to generate the figures will be archived in a public repository upon acceptance and a DOI will be provided in the final paper. All underlying sediment-core proxy series and the GISP2 temperature reconstruction used in this study are available from the cited sources. The exact input files used in this analysis will be archived alongside the code upon acceptance.

Author contributions. LNvdL, CSA and JHC conceived the study and supervised the student work of APK. APK developed the original code and wrote their B.Sc. thesis on the topic. LNvdL revised and reproduced the analysis and wrote the paper. JHC, CSA and APK edited the paper.

Competing interests. The authors declare no competing interests.

Acknowledgements. LNvdL, JHC and CSA acknowledge the Independent Research Fund Denmark (DFF) project Greenplanning (grant no. 0217-00244B). LNvdL also acknowledges the ARIA Forecasting Tipping Points Programme project G-PREWS (SCOP-PR01-P024). Finally, the author team acknowledges the National Snow and Ice Data Center QGreenland package. The authors also acknowledge the student work by Hongli Wu, which contributed to this manuscript.

https://doi.org/10.5194/egusphere-2026-3720
Preprint. Discussion started: 7 July 2026

References

Andersen, O. G. N.: The annual cycle of temperature, salinity, currents and water masses in Disko Bugt and adjacent waters, West Greenland, vol. 5, Museum Tusculanum Press, 1981.

Andresen, C. S., McCarthy, D. J., Valdemar Dylmer, C., Seidenkrantz, M.-S., Kuijpers, A., and Lloyd, J. M.: Interaction between subsurface ocean waters and calving of the Jakobshavn Isbræ during the late Holocene, The Holocene, 21, 211–224, https://doi.org/10.1177/0959683610378877, 2011.

Becker, F. and Blascheck, T.: TimeSeriesMaker: Interactive Time Series Composition in No Time, in: 2024 IEEE 17th Pacific Visualization Conference (PacificVis), pp. 301–306, IEEE, 2024.

Chelouah, R. and Siarry, P.: Genetic and Nelder–Mead algorithms hybridized for a more accurate global optimization of continuous multiminima functions, European Journal of operational research, 148, 335–348, 2003.

Delworth, T. L. and Mann, M. E.: Observed and simulated multidecadal variability in the Northern Hemisphere, Climate Dynamics, 16, 661–676, https://doi.org/10.1007/s003820000075, 2000.

Hanna, E., Jones, J. M., Cappelen, J., Mernild, S. H., Wood, L., Steffen, K., and Huybrechts, P.: The influence of North Atlantic atmospheric and oceanic forcing effects on 1900–2010 Greenland summer climate and ice melt/runoff, International Journal of Climatology, 33, 862–880, https://doi.org/10.1002/joc.3475, 2013.

Harff, B., Dietrich, R., Endler, R., Hentzsch, B., Jensen, J., Kuijpers, A., Krauss, N., Leipe, T., Lloyd, J., Mikkelsen, N., et al.: Deglaciation history, coastal development, and environmental change during the Holocene in western Greenland.: Cruise Report V7V MARIA S. MERIAN. Cruise MSM 05/03. June 15 to July 4, 2007, West Greenland, 2007.

Heaton, T. J., Köhler, P., Butzin, M., Bard, E., Reimer, R. W., Austin, W. E. N., Bronk Ramsey, C., Grootes, P. M., Hughen, K. A., Kromer, B., Reimer, P. J., Adkins, J., Burke, A., Cook, M. S., Olsen, J., and Skinner, L. C.: Marine20—The Marine Radiocarbon Age Calibration Curve (0–55,000 cal BP), Radiocarbon, 62, 779–820, https://doi.org/10.1017/rdc.2020.68, 2020.

Hurrell, J. W.: Decadal trends in the North Atlantic Oscillation: Regional temperatures and precipitation, Science, 269, 676–679, 1995.

Jakobsson, M., Mayer, L. A., Bringensparr, C., Castro, C. F., Mohammad, R., Johnsson, P., Ketter, T., Amblās i Novellas, D., Arndt, J. E., Canals Artigas, M., et al.: The International Bathymetric Chart of the Arctic Ocean (IBCAO) version 4.0, Scientific Data, 2020, vol. 7, num. 176, p. 1-14, 2020.

Kobashi, T., Severinghaus, J. P., and Kawamura, K.: Argon and nitrogen isotopes of trapped air in the GISP2 ice core during the Holocene epoch (0–11,500 BP): Methodology and implications for gas loss processes, Geochimica et Cosmochimica Acta, 72, 4675–4686, 2008.

Kobashi, T., Kawamura, K., Severinghaus, J. P., Barnola, J.-M., Nakaegawa, T., Vinther, B. M., Johnsen, S. J., and Box, J. E.: High variability of Greenland surface temperature over the past 4000 years estimated from trapped air in an ice core, Geophysical Research Letters, 38, 2011.

Lloyd, J., Moros, M., Perner, K., Telford, R. J., Kuijpers, A., Jansen, E., and McCarthy, D.: A 100 yr record of ocean temperature control on the stability of Jakobshavn Isbrae, West Greenland, Geology, 39, 867–870, 2011.

Meese, D. A., Gow, A. J., Alley, R. B., Zielinski, G. A., Grootes, P. M., Ram, M., Taylor, K. C., Mayewski, P. A., and Bolzan, J. F.: The Greenland Ice Sheet Project 2 depth-age scale: Methods and results, Journal of Geophysical Research: Oceans, 102, 26 411–26 423, https://doi.org/10.1029/97jc00269, 1997.

Moon, T. A., Fisher, M., Stafford, T., and Thurber, A.: QGreenland (v3), https://doi.org/10.5281/zenodo.12823307, 2023.

Murray, J. W.: Ecology and palaeoecology of benthic foraminifera, Routledge, https://doi.org/10.4324/9781315846101, 1991.

https://doi.org/10.5194/egusphere-2026-3720
Preprint. Discussion started: 7 July 2026

Nelder, J. A. and Mead, R.: A simplex method for function minimization, The computer journal, 7, 308–313, 1965.

Ouellet-Bernier, M.-M., de Vernal, A., Hillaire-Marcel, C., and Moros, M.: Paleoceanographic changes in the Disko Bugt area, West Greenland, during the Holocene, The Holocene, 24, 1573–1583, 2014.

Pearce, C., Özdemir, K. S., Forchhammer Mathiasen, R., Detlef, H., and Olsen, J.: The marine reservoir age of Greenland coastal waters, Geochronology, 5, 451–465, https://doi.org/10.5194/gchron-5-451-2023, 2023.

Perner, K., Moros, M., Lloyd, J., Kuijpers, A., Telford, R., and Harff, J.: Centennial scale benthic foraminiferal record of late Holocene oceanographic variability in Disko Bugt, West Greenland, Quaternary Science Reviews, 30, 2815–2826, 2011.

Perner, K., Moros, M., Jennings, A., Lloyd, J., and Knudsen, K.: Holocene palaeoceanographic evolution off West Greenland, The Holocene, 23, 374–387, https://doi.org/10.1177/0959683612460785, 2013.

Reimer, P. J., Bard, E., Bayliss, A., Beck, J. W., Blackwell, P. G., Ramsey, C. B., Buck, C. E., Cheng, H., Edwards, R. L., Friedrich, M., Grootes, P. M., Guilderson, T. P., Haflidason, H., Hajdas, I., Hatté, C., Heaton, T. J., Hoffmann, D. L., Hogg, A. G., Hughen, K. A., Kaiser, K. F., Kromer, B., Manning, S. W., Niu, M., Reimer, R. W., Richards, D. A., Scott, E. M., Southon, J. R., Staff, R. A., Turney, C. S. M., and van der Plicht, J.: IntCal13 and Marine13 Radiocarbon Age Calibration Curves 0–50,000 Years cal BP, Radiocarbon, 55, 1869–1887, https://doi.org/10.2458/azu_js_rc.55.16947, 2013.

Rytter, F., Knudsen, K. L., Seidenkrantz, M.-S., and Eiríksson, J.: Modern distribution of benthic foraminifera on the North Icelandic shelf and slope, The Journal of Foraminiferal Research, 32, 217–244, 2002.

Räth, C. and Monetti, R.: Surrogates with Random Fourier Phases, in: Topics on Chaotic Systems, p. 274–285, WORLD SCIENTIFIC, https://doi.org/10.1142/9789814271349_0031, 2009.

Salvador, S. and Chan, P.: Toward accurate dynamic time warping in linear time and space, Intelligent Data Analysis, 11, 561–580, https://doi.org/10.3233/ida-2007-11508, 2007.

Schlesinger, M. E. and Ramankutty, N.: An oscillation in the global climate system of period 65–70 years, Nature, 367, 723–726, https://doi.org/10.1038/367723a0, 1994.

Sejrup, H., Birks, H., Kristensen, D. K., and Madsen, H.: Benthonic foraminiferal distributions and quantitative transfer functions for the northwest European continental margin, Marine Micropaleontology, 53, 197–226, 2004.

Sha, L., Jiang, H., Seidenkrantz, M.-S., Knudsen, K. L., Olsen, J., Kuijpers, A., and Liu, Y.: A diatom-based sea-ice reconstruction for the Vaigat Strait (Disko Bugt, West Greenland) over the last 5000yr, Palaeogeography, Palaeoclimatology, Palaeoecology, 403, 66–79, https://doi.org/10.1016/j.palaeo.2014.03.028, 2014.

Vinther, B. M., Clausen, H. B., Johnsen, S. J., Rasmussen, S. O., Andersen, K. K., Buchardt, S. L., Dahl-Jensen, D., Seierstad, I. K., Siggaard-Andersen, M., Steffensen, J. P., Svensson, A., Olsen, J., and Heinemeier, J.: A synchronized dating of three Greenland ice cores throughout the Holocene, Journal of Geophysical Research: Atmospheres, 111, https://doi.org/10.1029/2005jd006921, 2006.

Wangner, D. J., Jennings, A. E., Vermassen, F., Dyke, L. M., Hogan, K. A., Schmidt, S., Kjær, K. H., Knudsen, M. F., and Andresen, C. S.: A 2000-year record of ocean influence on Jakobshavn Isbræ calving activity, based on marine sediment cores, The Holocene, 28, 1731–1744, https://doi.org/10.1177/0959683618788701, 2018.

Yeager, S. G. and Robson, J. I.: Recent Progress in Understanding and Predicting Atlantic Decadal Climate Variability, Current Climate Change Reports, 3, 112–127, https://doi.org/10.1007/s40641-017-0064-z, 2017.

https://doi.org/10.5194/egusphere-2026-3720
Preprint. Discussion started: 7 July 2026

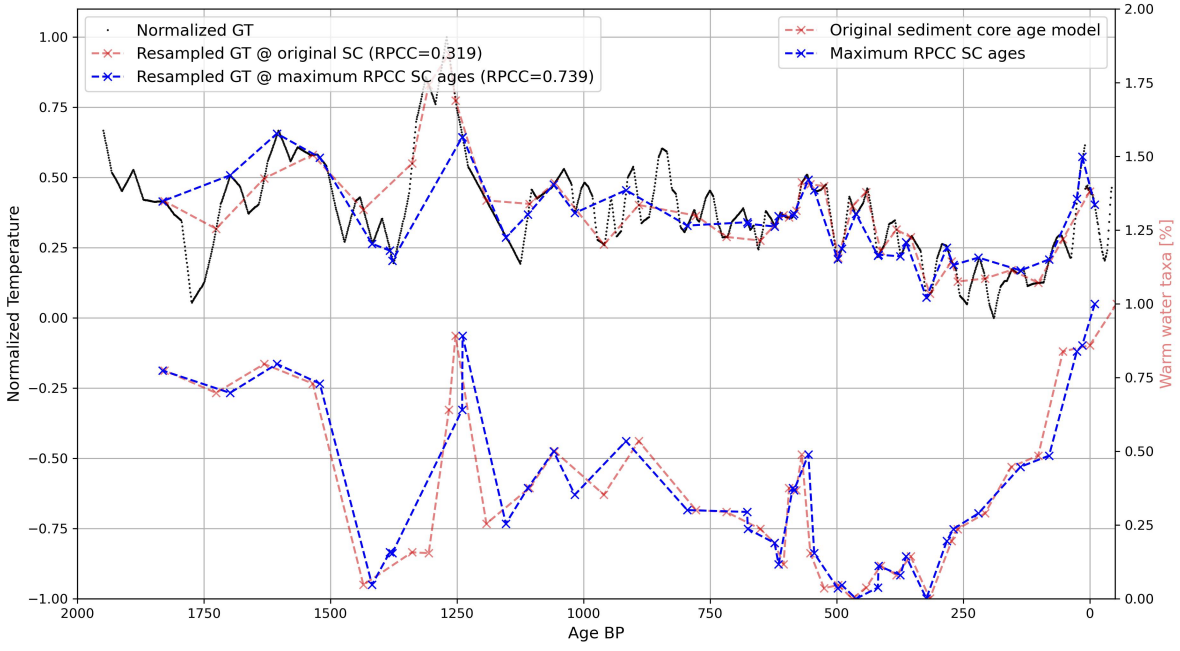

Figure A1. Nelder-Mead Optimization results for the Isfjeldsbanken core against the GISP2 time series.

Appendix A: Appendix A

This appendix includes the Nelder-Mead- and DTW-optimized time series plots for the remaining cores, against both the GISP2 ice core data and the random time series.

https://doi.org/10.5194/egusphere-2026-3720
Preprint. Discussion started: 7 July 2026

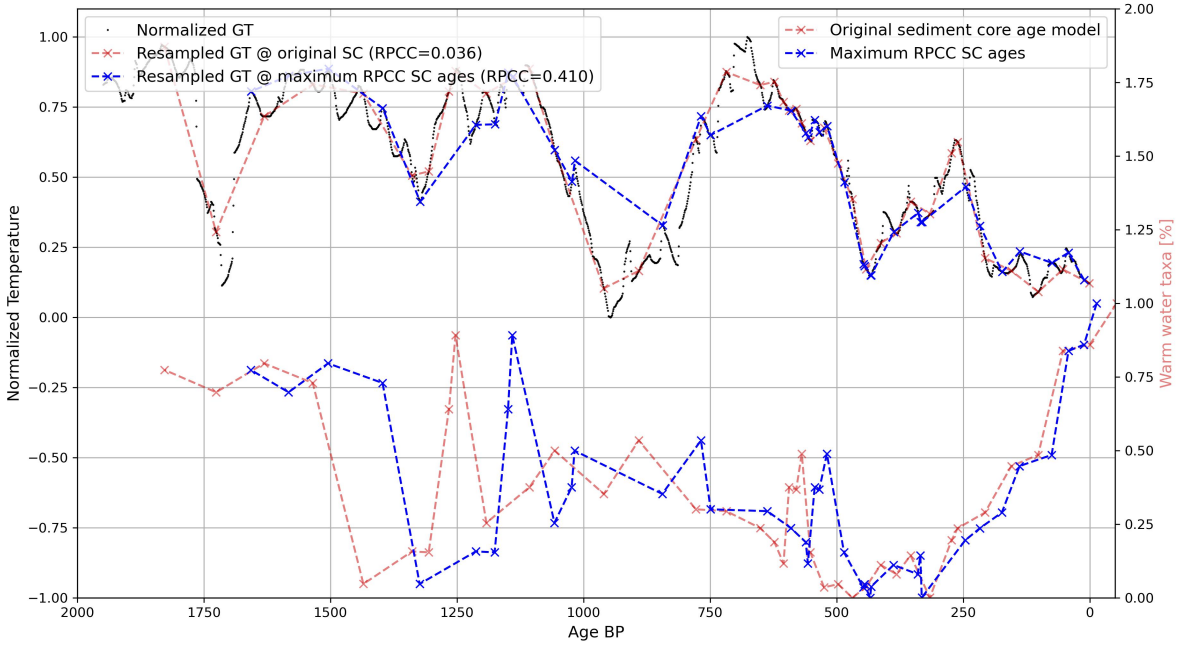

Figure A2. Nelder-Mead Optimization results for the Isfjeldsbanken core against a random time series.

https://doi.org/10.5194/egusphere-2026-3720
Preprint. Discussion started: 7 July 2026

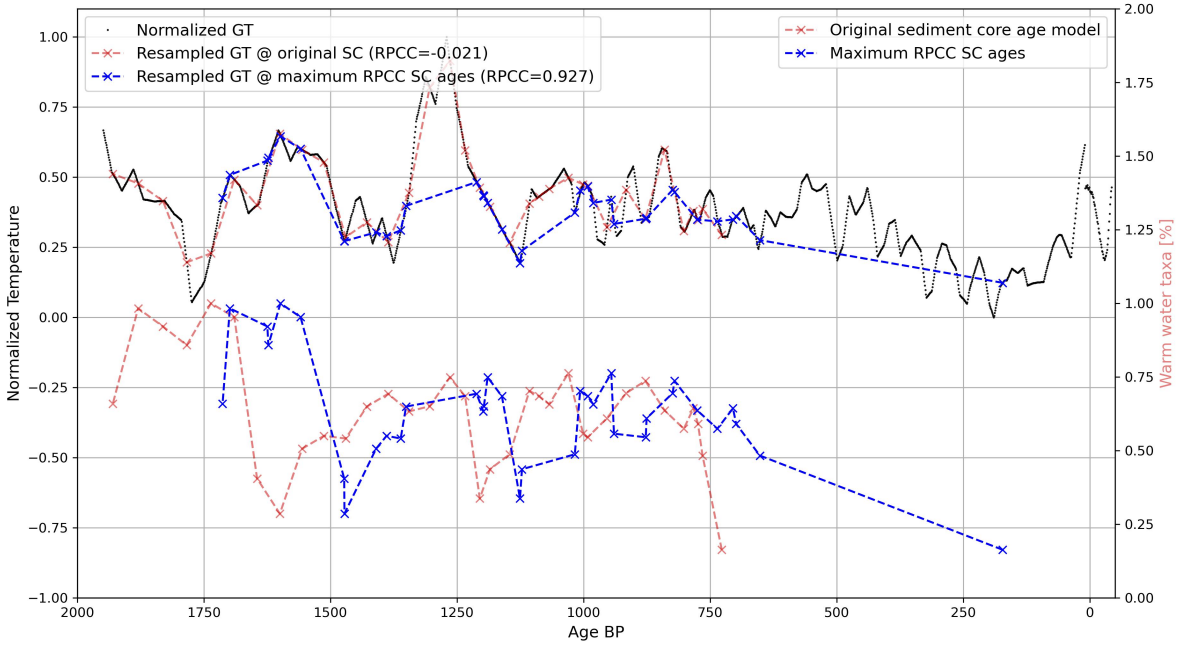

Figure A3. Nelder-Mead Optimization results for the Aasiaat 1 core against the GISP2 time series.

https://doi.org/10.5194/egusphere-2026-3720
Preprint. Discussion started: 7 July 2026

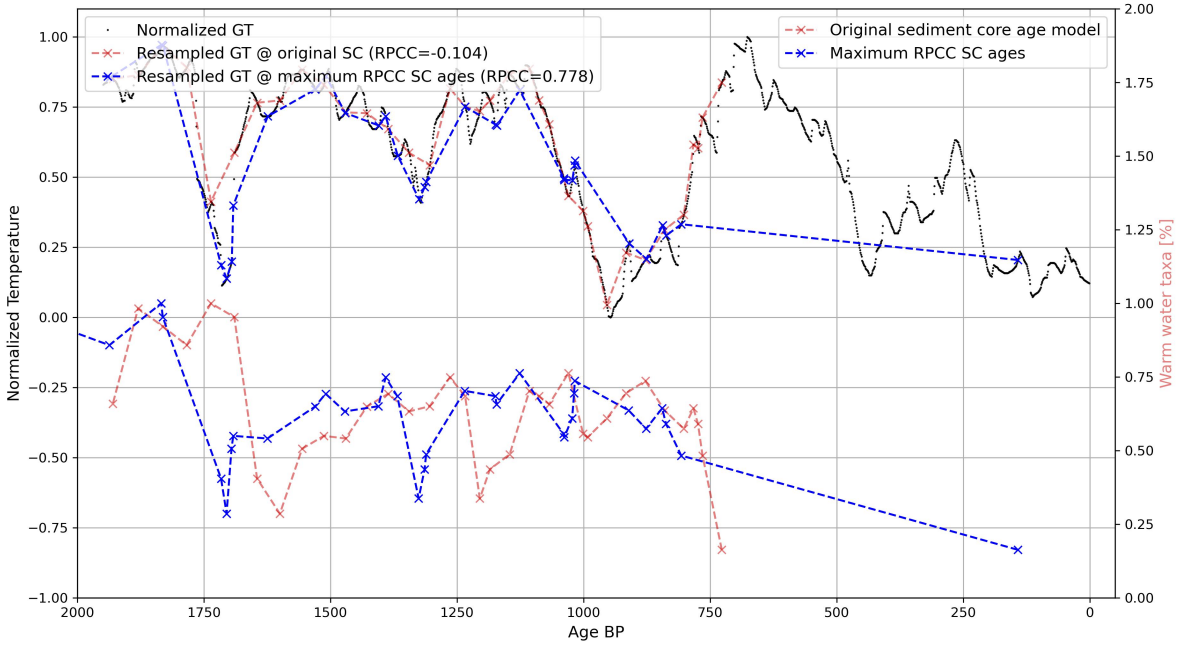

Figure A4. Nelder-Mead Optimization results for the Aasiaat 1 core against a random time series.

https://doi.org/10.5194/egusphere-2026-3720
Preprint. Discussion started: 7 July 2026

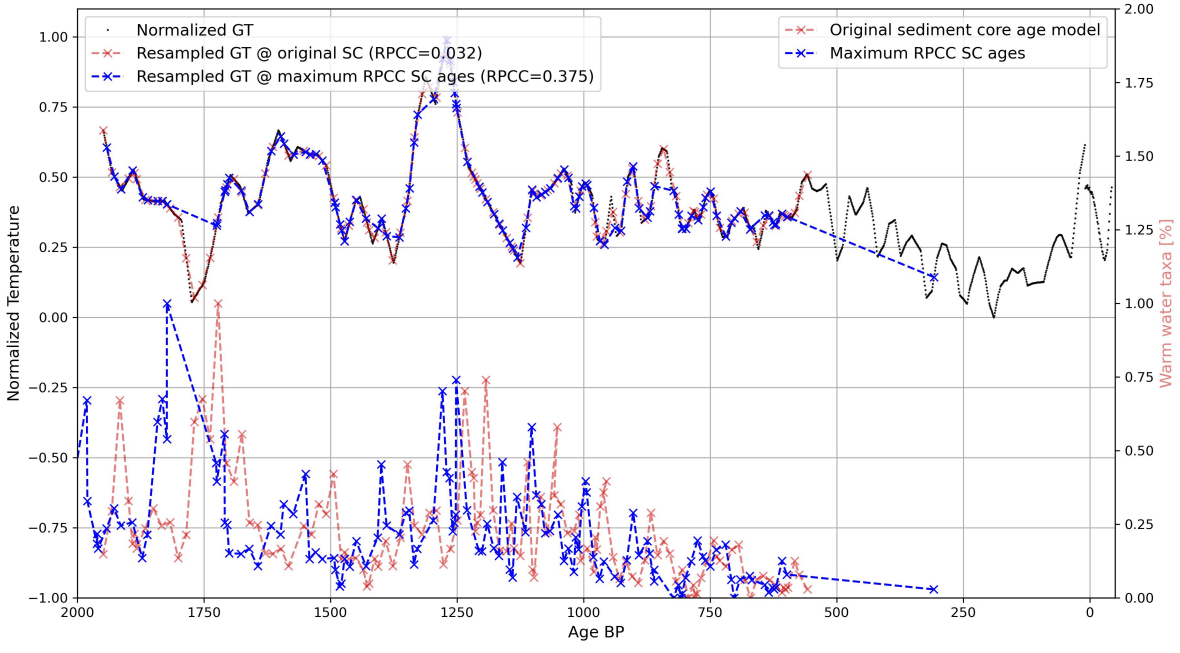

Figure A5. Nelder-Mead Optimization results for the Aasiaat 2 core against the GISP2 time series.

https://doi.org/10.5194/egusphere-2026-3720
Preprint. Discussion started: 7 July 2026

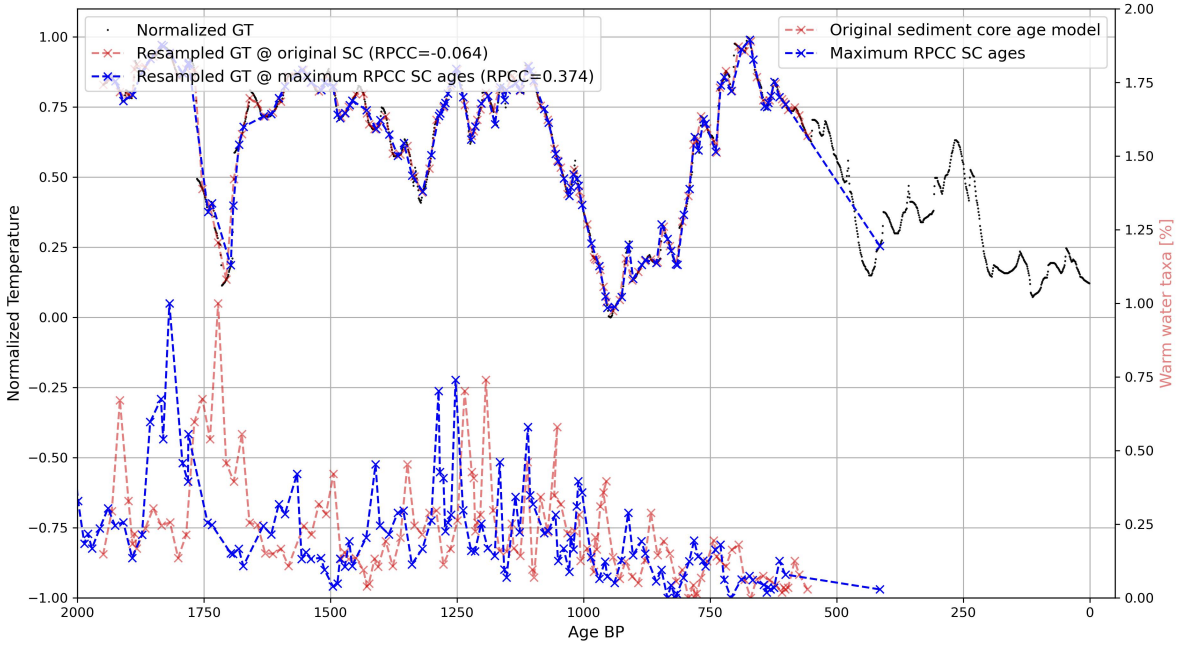

Figure A6. Nelder-Mead Optimization results for the Aasiaat 2 core against a random time series.

https://doi.org/10.5194/egusphere-2026-3720
Preprint. Discussion started: 7 July 2026

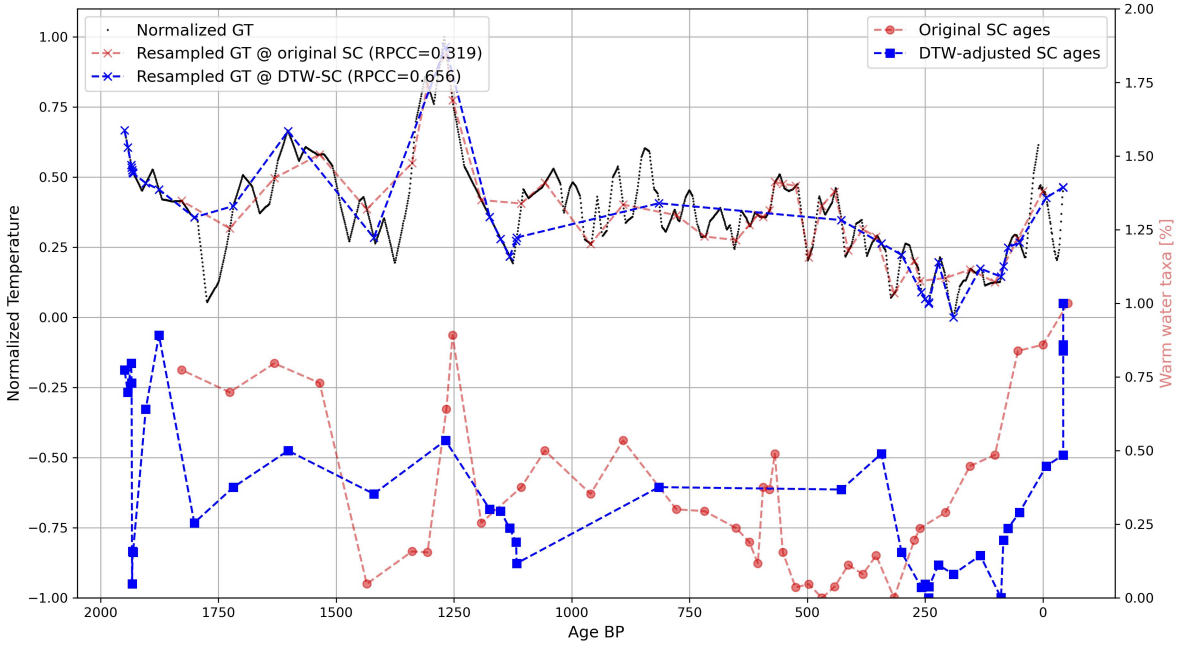

Figure A7. Dynamic Time Warping results for the Isfjeldsbanken core against the GISP2 time series.

https://doi.org/10.5194/egusphere-2026-3720
Preprint. Discussion started: 7 July 2026

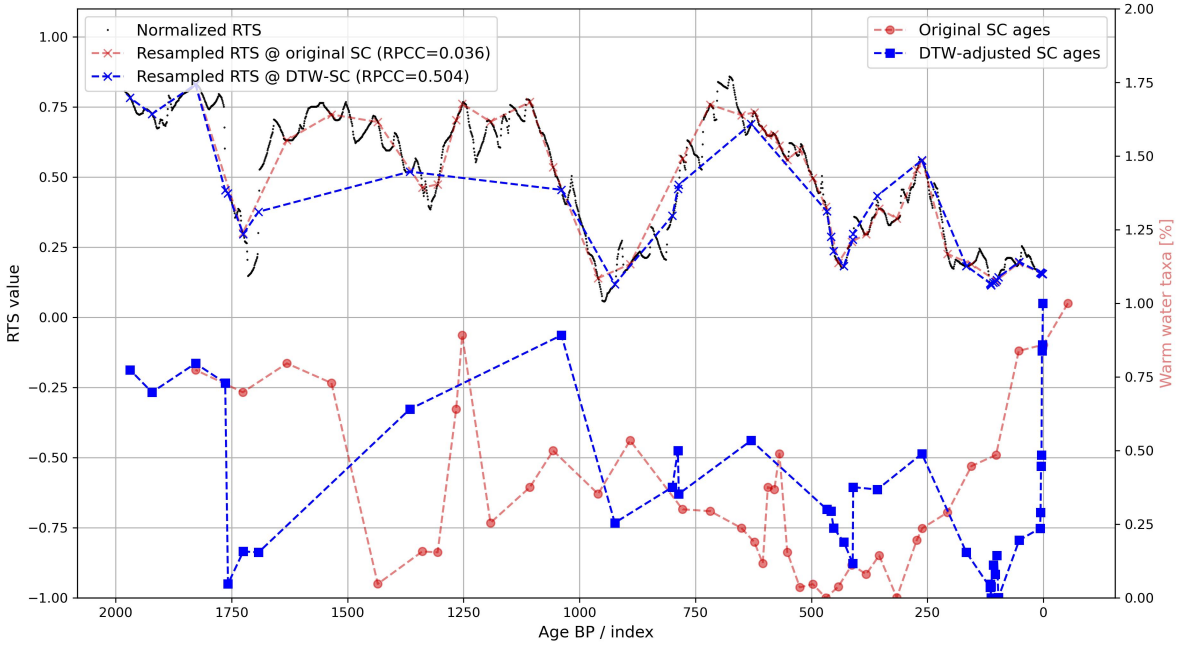

Figure A8. Dynamic Time Warping results for the Isfjeldsbanken core against a random time series.

https://doi.org/10.5194/egusphere-2026-3720
Preprint. Discussion started: 7 July 2026

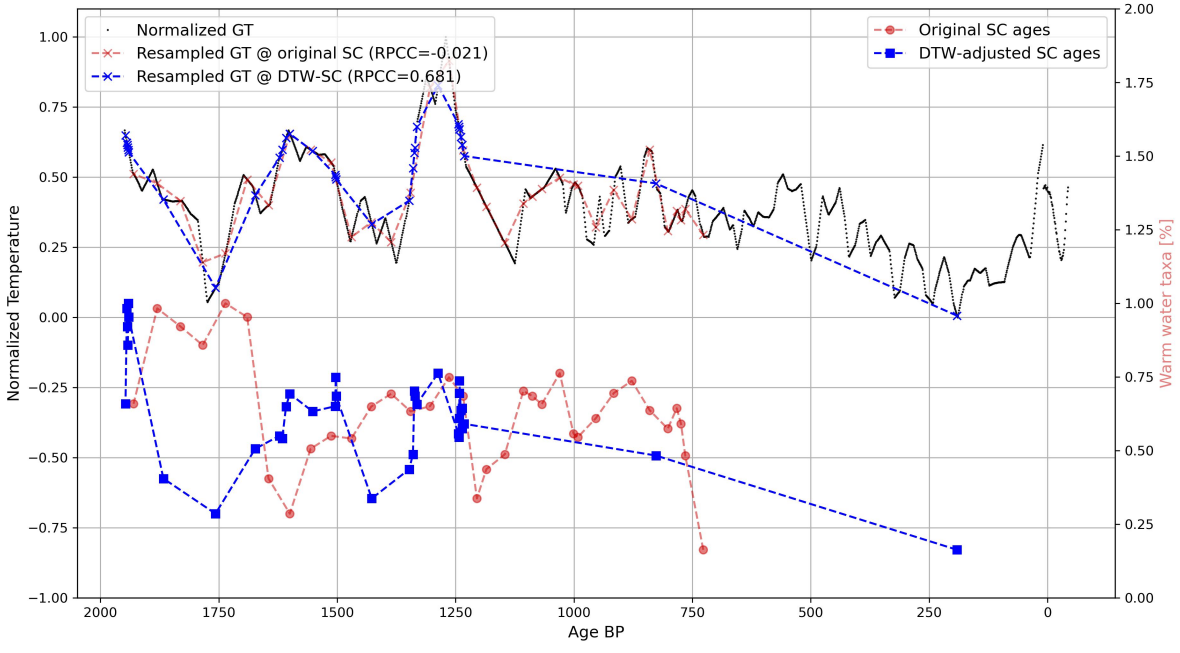

Figure A9. Dynamic Time Warping results for the Aasiaat 1 core against the GISP2 time series.

https://doi.org/10.5194/egusphere-2026-3720
Preprint. Discussion started: 7 July 2026

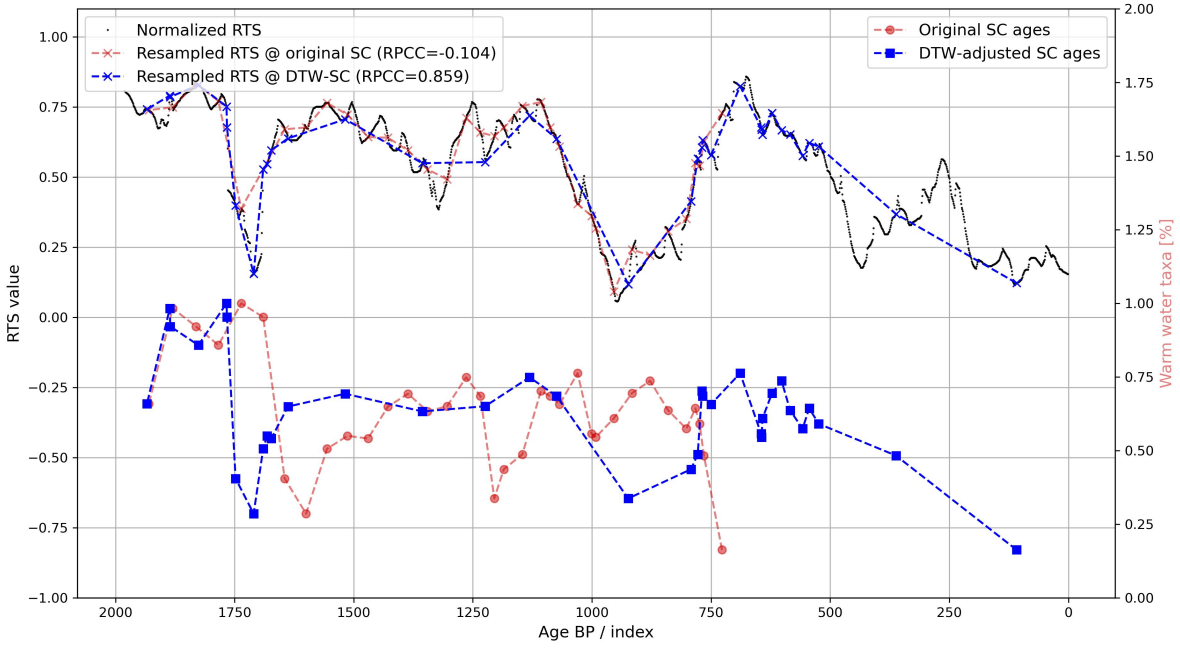

Figure A10. Dynamic Time Warping results for the Aasiaat 1 core against a random time series.

https://doi.org/10.5194/egusphere-2026-3720
Preprint. Discussion started: 7 July 2026

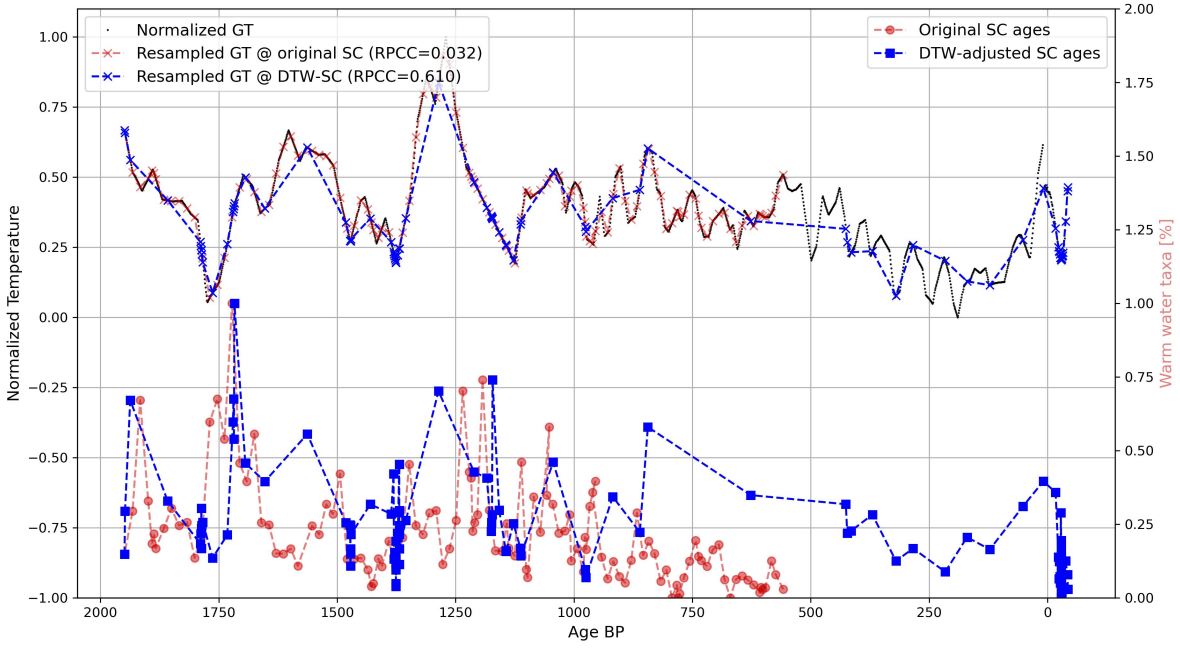

Figure A11. Dynamic Time Warping results for the Aasiaat 2 core against the GISP2 time series.

https://doi.org/10.5194/egusphere-2026-3720
Preprint. Discussion started: 7 July 2026

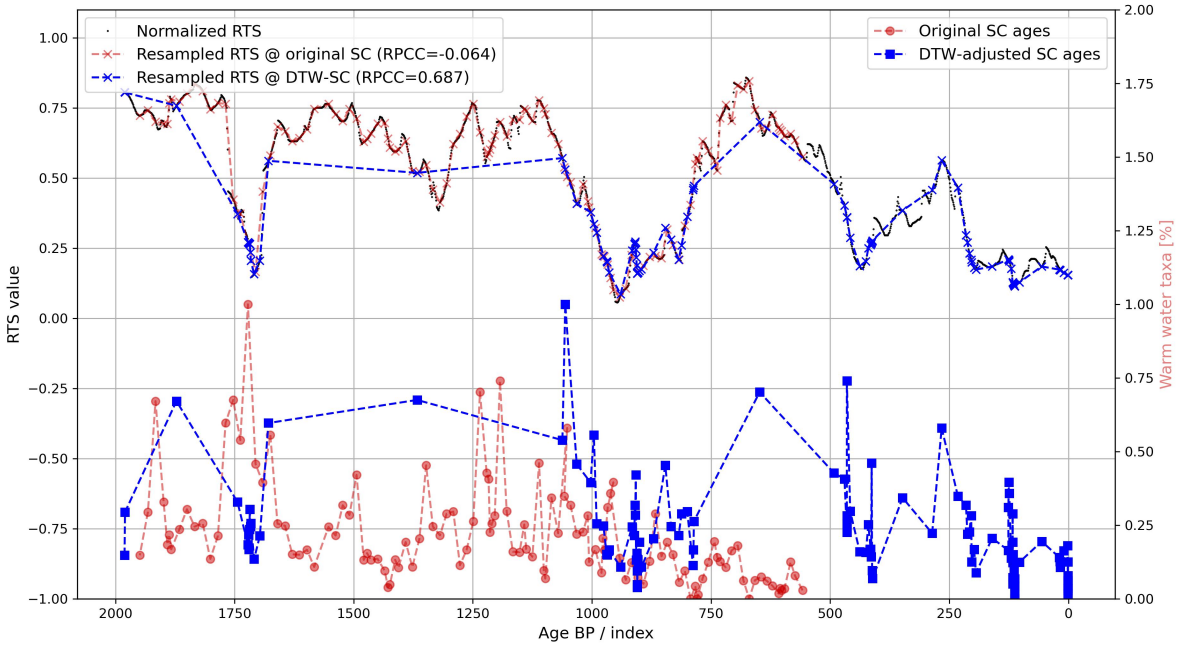

Figure A12. Dynamic Time Warping results for the Aasiaat 2 core against a random time series.